

Impact of Rotation on the Structure and Composition of Neutron Stars

Fridolin Weber

Department of Physics, San Diego State University, San Diego, California 92182, USA & Center for Astrophysics and Space Sciences, University of California, San Diego, La Jolla, California 92093, USA

Email: fweber@mail.sdsu.edu

*Milva Orsaria*¹

Department of Physics, San Diego State University, San Diego, CA 92182, USA

Email: morsaria@rohan.sdsu.edu

Rodrigo Negreiros

Instituto de Física, Universidade Federal Fluminense, Niterói, RJ, Brazil

Email: negreiros@if.uff.br

1 Introduction

Depending on mass and rotational frequency, gravity compresses the matter in the core regions of neutron stars to densities that are several times higher than the density of ordinary atomic nuclei [1, 2, 3, 4, 5, 6, 7, 8, 9]. At such huge densities atoms themselves collapse, and atomic nuclei are squeezed so tightly together that new particle states may appear and novel states of matter, foremost quark matter, may be created. This feature makes neutron stars superb astrophysical laboratories for a wide range of physical studies [1, 2, 3, 4, 6, 8, 10]. And with observational data accumulating rapidly from both orbiting and ground based observatories spanning the spectrum from X-rays to radio wavelengths, there has never been a more exiting time than today to study neutron stars. The Hubble Space Telescope and X-ray satellites such as Chandra and XMM-Newton in particular have proven especially valuable. New astrophysical instruments such as the Five hundred meter Aperture Spherical Telescope (FAST), the square kilometer Array (skA), Fermi Gamma-ray Space Telescope (formerly GLAST), and possibly the International X-ray Observatory (now Advanced Telescope for High ENergy Astrophysics, ATHENA) promise the discovery of tens of thousands of new non-rotating and rotating neutron stars. The latter are referred to as pulsars. This paper provides a short overview of the impact of

¹Home address: CONICET, Rivadavia 1917, 1033 Buenos Aires, Argentina;
Gravitation, Astrophysics and Cosmology Group, Facultad de Ciencias Astronómicas y Geofísicas,
Paseo del Bosque S/N (1900), Universidad Nacional de La Plata UNLP, La Plata, Argentina

rotation on the structure and composition of neutron stars. Observational properties, which may help to shed light on the core composition of neutron stars—and, hence, the properties of ultra-dense matter [11, 12]—are discussed.

2 Modeling of Rotating Neutron Stars

The structure equations of rotating neutron stars are based on a line element of the form [2, 13, 14, 15, 16, 17, 18]

$$ds^2 = -e^{2\nu} dt^2 + e^{2\psi} (d\phi - \omega dt)^2 + e^{2\mu} d\theta^2 + e^{2\lambda} dr^2, \quad (1)$$

where each metric function, ν , ψ , μ and λ , as well as the angular velocities of the local inertial frames, ω , depend on the radial coordinate r and on the polar angle θ and, implicitly, on the star's angular velocity Ω . The metric functions and the frame dragging frequency are to be computed from Einstein's field equation,

$$G^{\alpha\beta} \equiv R^{\alpha\beta} - \frac{1}{2} R g^{\alpha\beta} = 8\pi T^{\alpha\beta}, \quad (2)$$

where $T^{\alpha\beta} = T^{\alpha\beta}(\epsilon, P(\epsilon))$ denotes the energy momentum tensor of the stellar matter whose equation of state is given by $P(\epsilon)$. No simple stability criteria are known for rapidly rotating stellar configurations in general relativity. However, an absolute limit on rapid rotation is set by the onset of mass shedding from the equator of a rotating star. The corresponding rotational frequency is known as the Kepler frequency, Ω_K . In classical mechanics, the expression for the Kepler frequency, determined by the equality between the centrifugal force and gravity, is readily obtained as $\Omega_K = \sqrt{M/R^3}$. Its general relativistic counterpart is given by [2, 13]

$$\Omega_K = \omega + \frac{\omega_{,r}}{2\psi_{,r}} + e^{\nu-\psi} \sqrt{\frac{\nu_{,r}}{\psi_{,r}} + \left(\frac{\omega_{,r}}{2\psi_{,r}} e^{\psi-\nu}\right)^2}, \quad (3)$$

which is to be evaluated self-consistently at the equator of a rotating neutron star. The Kepler period follows from Eq. (3) as $P_K = 2\pi/\Omega_K$. For typical neutron star matter equations of state, the Kepler period obtained for $1.4 M_\odot$ neutron stars is around 1 ms (Fig. 1) [2, 5, 13, 14]. An exception to this are strange quark matter stars. Since they are self-bound, they tend to possess smaller radii than conventional neutron stars, which are bound by gravity only. Because of their smaller radii, strange stars can withstand mass shedding from the equator down to periods of around 0.5 ms [19, 20].

A mass increase of up to $\sim 20\%$ is typical for rotation at Ω_K . Because of rotation, the equatorial radii increase by several kilometers, while the polar radii become smaller by several kilometers. The ratio between both radii is around 2/3, except

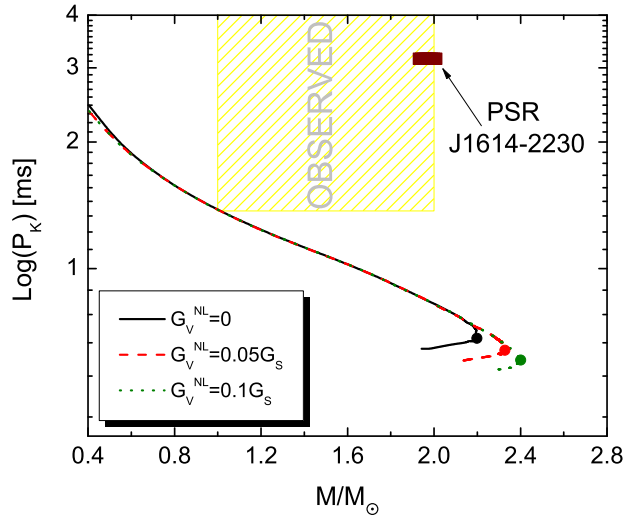


Figure 1: Kepler period, P_K , of a sequence of rotating neutron stars computed for the NJL equation of state discussed in Section 4. The colored solid dots denote the termination point of each stellar sequence, which depends on the stiffness (i.e. G_V^{NL} value) of the equation of state.

for rotation close to the Kepler frequency. The most rapidly rotating, currently known neutron star is pulsar PSR J1748-2446ad, which rotates at a period of 1.39 ms (719 Hz) [21], well below the Kepler frequency for most neutron star equations of state. Examples of other rapidly rotating neutron stars are PSRs B1937+21 [22] and B1957+20 [23], whose rotational periods are 1.58 ms (633 Hz) and 1.61 ms (621 Hz), respectively.

The density change in the core of a neutron star whose frequency varies from $0 \leq \Omega \leq \Omega_K$ can be as large as 60% [2, 5]. This suggests that rotation may drive phase transitions or cause significant compositional changes of the matter in the cores of neutron stars. Examples of the latter are shown in Figs. 2 and 3, which illustrate rotation-driven changes in the hyperon compositions of neutron stars. Qualitatively similar restructuring effects are obtained if neutron stars should contain deconfined quark matter in their cores [1, 2, 5]. Quantitatively, however, there may be a striking difference if quark matter is present, which could lead to a “backbending” of pulsars [24]. In the latter case, quark deconfinement may register itself in the braking index n , which could be somewhere between $-\infty < n < +\infty$ rather than $n \approx 3$, as well as in the spin-ups of isolated pulsars, which could last from tens of thousands to hundreds of thousands of years [5, 24].

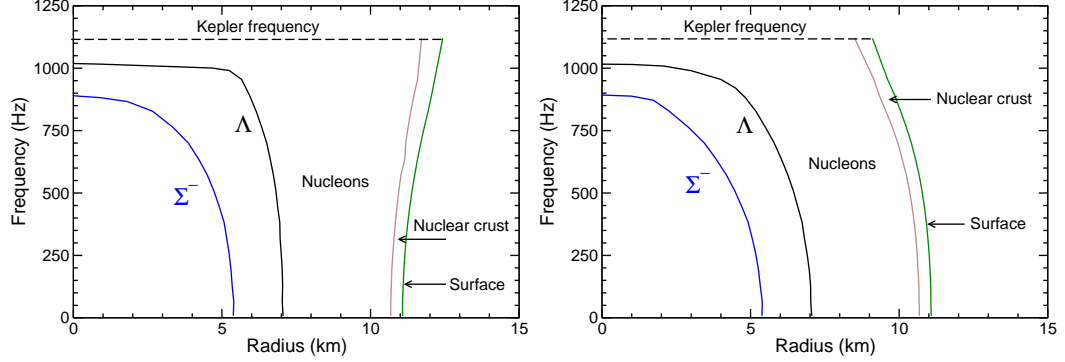


Figure 2: Composition of a rotating neutron star in equatorial direction (left panel) and polar direction (right panel) [2, 25]. The star’s mass at zero rotation is $1.40 M_{\odot}$.

3 Core Composition of Rotating Neutron Stars

The hadronic phase inside of neutron stars may be described in the framework of non-linear relativistic nuclear field theory [1, 2], where baryons (neutrons, protons, hyperons) interact via the exchange of scalar, vector and isovector mesons (σ , ω , $\vec{\rho}$, respectively). The Lagrangian of the theory is given by

$$\begin{aligned}
\mathcal{L} = & \sum_{B=n,p,\Lambda,\Sigma,\Xi} \bar{\psi}_B [\gamma_{\mu} (i\partial^{\mu} - g_{\omega}\omega^{\mu} - g_{\rho}\vec{\rho}^{\mu}) - (m_N - g_{\sigma}\sigma)] \psi_B + \frac{1}{2} (\partial_{\mu}\sigma\partial^{\mu}\sigma - m_{\sigma}^2\sigma^2) \\
& - \frac{1}{3} b_{\sigma} m_N (g_{\sigma}\sigma)^3 - \frac{1}{4} c_{\sigma} (g_{\sigma}\sigma)^4 - \frac{1}{4} \omega_{\mu\nu} \omega^{\mu\nu} + \frac{1}{2} m_{\omega}^2 \omega_{\mu}\omega^{\mu} + \frac{1}{2} m_{\rho}^2 \vec{\rho}_{\mu} \cdot \vec{\rho}^{\mu} \\
& - \frac{1}{4} \vec{\rho}_{\mu\nu} \vec{\rho}^{\mu\nu} + \sum_{\lambda=e^{-},\mu^{-}} \bar{\psi}_{\lambda} (i\gamma_{\mu}\partial^{\mu} - m_{\lambda}) \psi_{\lambda},
\end{aligned} \tag{4}$$

where B sums all baryon states which become populated in neutron star matter [1, 2]. The quantities g_{ρ} , g_{σ} , and g_{ω} are the meson-baryon coupling constants. Non-linear σ -meson self-interactions are taken into account in Eq. (4) via the terms proportional to b_{σ} and c_{σ} . The equations of motion for the baryon and meson field equations, which follow from Eq. (4), can be solved using the relativistic mean-field approximation, where the meson fields are approximated by their respective mean-field values $\bar{\sigma} \equiv \langle \sigma \rangle$, $\bar{\omega} \equiv \langle \omega \rangle$, and $\bar{\rho}_{03} \equiv \langle \rho_{03} \rangle$ [1, 2]. The parameters of the model are adjusted to the properties of nuclear matter at saturation density. Figures 2 and 3 show the compositions of rotating neutron stars based on the Lagrangian of Eq. (4). One sees that, depending on the mass of a neutron, certain hyperon species may not be present at high neutron star rotation rates.

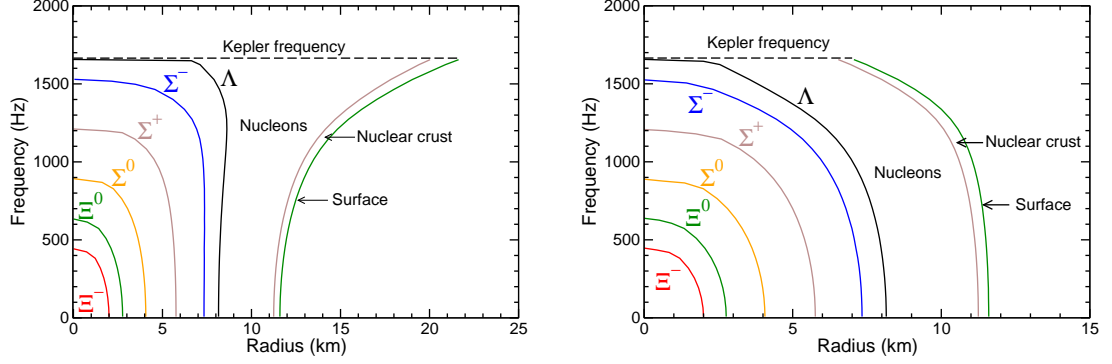


Figure 3: Same as Figure 2, but for a non-rotating stellar mass of $1.70 M_{\odot}$ [2, 26].

4 Quark Matter in the Cores of Neutron Stars

Whether or not quark matter exists in the cores of neutron stars is an open issue. The observation of neutron stars with masses of up to around $2 M_{\odot}$ does not yet rule out quark matter [27, 28]. To model quark deconfinement, one may start from the Euclidean effective action associated with the nonlocal SU(3) quark model (for details, see [28] and references therein),

$$\begin{aligned}
S_E &= \int d^4x \{ \bar{\psi}(x) [-i\gamma_{\mu}\partial_{\mu} + \hat{m}] \psi(x) - \frac{G_s}{2} [j_a^S(x) j_a^S(x) + j_a^P(x) j_a^P(x)] \\
&\quad - \frac{H}{4} T_{abc} [j_a^S(x) j_b^S(x) j_c^S(x) - 3 j_a^S(x) j_b^P(x) j_c^P(x)] - \frac{G_V^{NL}}{2} j_{V,f}^{\mu}(x) j_{V,f}^{\mu}(x) \}, \quad (5)
\end{aligned}$$

where ψ is a chiral $U(3)$ vector that includes the light quark fields, $\psi \equiv (u \ d \ s)^T$, and $\hat{m} = \text{diag}(m_u, m_d, m_s)$ stands for the current quark mass matrix. For simplicity we consider the isospin symmetry limit so that $m_u = m_d = \bar{m}$. The fermion kinetic term includes the covariant derivative $D_{\mu} \equiv \partial_{\mu} - iA_{\mu}$, where A_{μ} are color gauge fields, and the operator $\gamma_{\mu}\partial_{\mu}$ in Euclidean space is defined as $\vec{\gamma} \cdot \vec{\nabla} + \gamma_4 \frac{\partial}{\partial \tau}$, with $\gamma_4 = i\gamma_0$. The currents $j_a^{S,P}(x)$ and $j_{V,f}^{\mu}(x)$ are defined in [28]. Using the mean-field approximation, one obtains from Eq. (5) the grand canonical potential

$$\begin{aligned}
\Omega^{NL}(T=0, \mu_f) &= -\frac{N_c}{\pi^3} \sum_{f=u,d,s} \int_0^{\infty} dp_0 \int_0^{\infty} dp \ln \left\{ [\omega_f^2 + M_f^2(\omega_f^2)] \frac{1}{\omega_f^2 + m_f^2} \right\} \\
&\quad - \frac{N_c}{\pi^2} \sum_{f=u,d,s} \int_0^{\sqrt{\tilde{\mu}_f^2 - m_f^2}} dp p^2 [(\tilde{\mu}_f - E_f) \theta(\tilde{\mu}_f - m_f)] \\
&\quad - \frac{1}{2} \left[\sum_{f=u,d,s} (\bar{\sigma}_f \bar{S}_f + \frac{G_s}{2} \bar{S}_f^2) + \frac{H}{2} \bar{S}_u \bar{S}_d \bar{S}_s \right] - \sum_{f=u,d,s} \frac{\varpi_{V,f}^2}{4G_V^{NL}}, \quad (6)
\end{aligned}$$

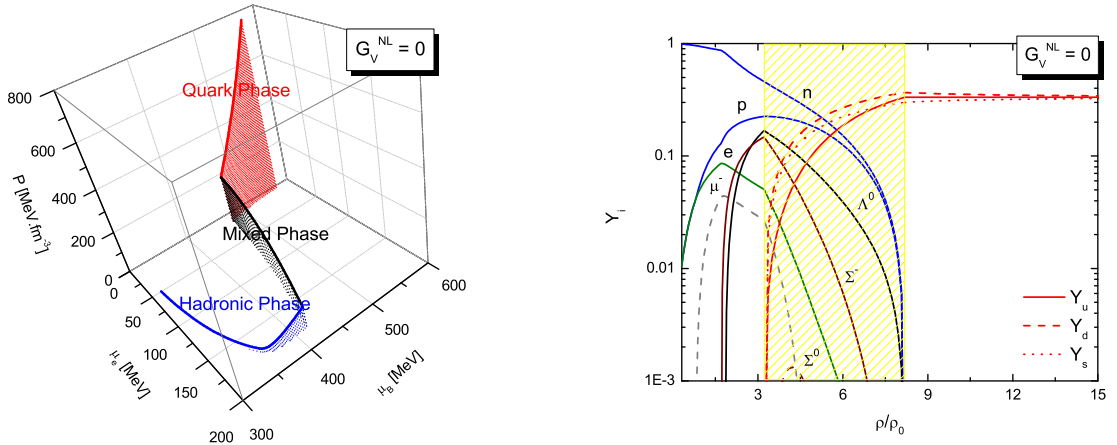


Figure 4: Equation of state (left panel) and associated quark-lepton composition (right panel) computed for $G_V^{NL} = 0$.

where $N_c = 3$, $E_f = \sqrt{\vec{p}^2 + m_f^2}$, and $\omega_f^2 = (p_0 + i\mu_f)^2 + \vec{p}^2$. The masses of free quarks are denoted by m_f , where $f = u, d, s$. The momentum-dependent constituent quark masses M_f depend explicitly on the quark mean fields $\bar{\sigma}_f$, $M_f(\omega_f^2) = m_f + \bar{\sigma}_f g(\omega_f^2)$, where $g(\omega^2)$ denotes the Fourier transform of the form factor $\tilde{g}(z)$. For a Gaussian form factor one has $g(\omega^2) = \exp(-\omega^2/\Lambda^2)$, where Λ plays a role for the stiffness of the chiral transition. This parameter, together with the current quark mass \bar{m} of up and down quarks and the coupling constants G_s and H in Eq. (6), have been fitted to the pion decay constant, f_π , and meson masses m_π , m_η , and $m_{\eta'}$ [28]. The result of this fit is $\bar{m} = 6.2$ MeV, $\Lambda = 706.0$ MeV, $G_s\Lambda^2 = 15.04$, $H\Lambda^5 = -337.71$. The strange quark current mass is treated as a free parameter and was set to $m_s = 140.7$ MeV. Using these parametrizations, the fields $\bar{\sigma}_f$ and $\varpi_{V,f}$ can be determined by minimizing Eq. (6), $\partial\Omega^{NL}/\partial\bar{\sigma}_f = \partial\Omega^{NL}/\partial\varpi_{V,f} = 0$. The strength of the vector interaction G_V is usually expressed in terms of the strong coupling constant G_s . To account for the uncertainty in the theoretical predictions for the ratio G_V/G_s , the vector coupling constant may be treated as a free parameter which varies from 0 to $0.1 G_s$.

To model the mixed phase region of quarks and hadrons in neutron stars, we use the Gibbs condition for phase equilibrium between hadronic (H) and quark (Q) matter,

$$P_H(\mu_n, \mu_e, \{\phi\}) = P_Q(\mu_n, \mu_e), \quad (7)$$

where P_H and P_Q denote the pressures of hadronic matter and quark matter, respectively [29, 30]. The quantity $\{\phi\}$ in Eq. (7) stands collectively for the field variables

$(\bar{\sigma}, \bar{\omega}, \bar{\rho})$ and Fermi momenta (k_B, k_λ) that characterize a solution to the equations of confined hadronic matter (Sect. 3). We use the symbol $\chi \equiv V_Q/V$ to denote the volume proportion of quark matter, V_Q , in the unknown volume V . By definition, χ then varies between 0 and 1, depending on how much confined hadronic matter has been converted to quark matter. Equation (7) is to be supplemented with the conditions of global baryon charge conservation and global electric charge conservation. The global conservation of baryon charge is expressed as [29, 30]

$$\rho_b = \chi \rho_Q(\mu_n, \mu_e) + (1 - \chi) \rho_H(\mu_n, \mu_e, \{\phi\}), \quad (8)$$

where ρ_Q and ρ_H denote the baryon number densities of the quark phase and hadronic phase, respectively. The global neutrality of electric charge is given by [29, 30]

$$0 = \chi q_Q(\mu_n, \mu_e) + (1 - \chi) q_H(\mu_n, \mu_e, \{\phi\}), \quad (9)$$

with q_Q and q_H denoting the electric charge densities of the quark phase and hadronic phase, respectively. We have chosen global rather than local electric charge neutrality. Local NJL studies carried out for local electric charge neutrality have been reported recently in Refs. [31, 32]. Figure 4 shows a model quark hadron composition and its associated equation of state computed for the nonlocal NJL model. A model composition for the mixed phase region is shown in Fig. 5. The inclusion of the quark vector coupling contribution shifts the onset of the phase transition to higher densities, and also narrows the width of the mixed quark-hadron phase, when compared to the case $G_V = 0$. The mixed phases range from $3.2 - 8.2\rho_0$, $3.8 - 8.5\rho_0$, and $4.5 - 8.9\rho_0$ for vector coupling constants $G_V/G_s = 0, 0.05, 0.1$, respectively. We note that there is considerable theoretical uncertainty in the ratio of G_V/G_s [33] since a rigorous derivation of the effective couplings from QCD is not possible. Combining the ratios of G_V/G_s from the molecular instanton liquid model and from the Fierz transformation, the value of G_V/G_s is expected to be in the range $0 \leq G_V/G_s \leq 0.5$ [34]. For our model, values of $G_V/G_s > 0.1$ shift the onset of the quark-hadron phase transition to such high densities that quark deconfinement can no longer occur in the cores of neutron stars.

As shown in [28], the maximum neutron star masses increase from $1.87 M_\odot$ for $G_V = 0$, to $2.00 M_\odot$ for $G_V = 0.05 G_s$, to $2.07 M_\odot$ for $G_V = 0.1 G_s$. The heavier stars of all three stellar sequences contain mixed phases of quarks and hadrons in their centers. The densities in these stars are however not high enough to generate pure quark matter in the cores. Such matter forms only in neutron stars which are already located on the gravitationally unstable branch of the mass-radius relationships. Another intriguing feature of this model is that neutron stars with canonical masses of around $1.4 M_\odot$ do not possess a mixed phase of quarks and hadrons but are made entirely of confined hadronic matter.

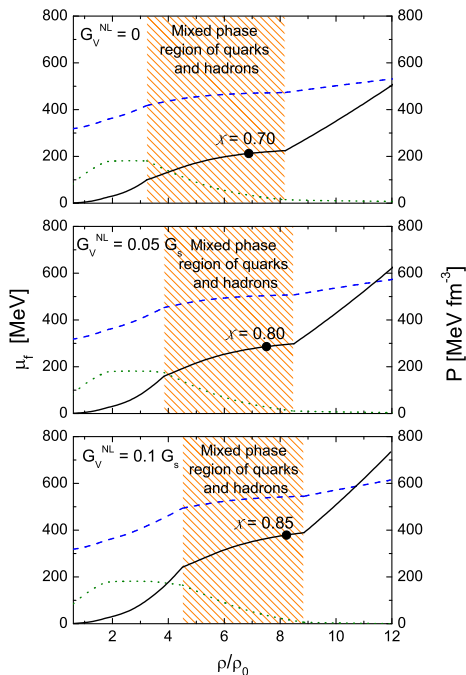


Figure 5: Pressure, P (solid lines), baryon chemical potential, μ_b (dashed lines), and electron chemical potential, μ_e (dotted lines) as a function of baryon number density, ρ , in units of the normal nuclear matter density, $\rho_0 = 0.16 \text{ fm}^{-3}$. The hatched areas denote the mixed phase regions where confined hadronic matter and deconfined quark matter coexist. The solid dots indicate the central densities of the associated maximum-mass stars, and χ is the respective fraction of quark matter inside of them. The results are shown for three different values of the vector coupling constant, ranging from 0, to $0.05 G_s$, to $0.1 G_s$. (Figure from Ref. [28].)

5 Thermal evolution of rotating neutron stars

The basic cooling features of a neutron star are easily grasped by considering the energy conservation relation of the star in the Newtonian limit [35]. This equation is given by

$$dE_{\text{th}}/dt = C_V dT/dt = -L_\nu - L_\gamma + H, \quad (10)$$

where E_{th} is the thermal energy content of a neutron star, T its internal temperature, and C_V its total specific heat. The energy sinks are the total neutrino luminosity, L_ν , and the surface photon luminosity, L_γ . The source term H includes all possible heating mechanisms [35], which, for instance, convert magnetic or rotational energy into heat. The dominant contributions to C_V come from the core whose constituents are

leptons, baryons, boson condensates and possibly deconfined superconducting quarks. When baryons and quarks become paired, their contribution to C_V is strongly suppressed at temperatures smaller than the critical temperatures associated with these pairing phases. The crustal contribution is in principle dominated by the free neutrons in the inner stellar crust but, since these are extensively paired, practically only the nuclear lattice and electrons contribute. Extensive baryon, and quark, pairing can thus significantly reduce C_V . In order to derive the general relativistic version of Eq. (10) for rotating stars, one needs to solve Einstein's field equations using the metric of a rotationally deformed fluid defined in Eq. (1). The result is the following parabolic differential equation,

$$\begin{aligned} \partial_t \tilde{T} = & -\frac{1}{\Gamma^2} e^{2\nu} \frac{\epsilon}{C_V} - r \sin \theta U e^{\nu+\gamma-\xi} \frac{1}{C_V} \left(\partial_r \Omega + \frac{1}{r} \partial_\theta \Omega \right) \\ & + \frac{1}{r^2 \sin \theta \Gamma} e^{3\nu-\gamma-2\xi} \frac{1}{C_V} \left(\partial_r \left(r^2 \kappa \sin \theta e^\gamma \left(\partial_r \tilde{T} + \Gamma^2 U e^{-2\nu+\gamma} \tilde{T} \partial_r \Omega \right) \right) \right. \\ & \left. + \frac{1}{r^2} \partial_\theta \left(r^2 \kappa \sin \theta e^\gamma \left(\partial_\theta \tilde{T} + \Gamma^2 U e^{-2\nu+\gamma} \tilde{T} \partial_\theta \Omega \right) \right) \right), \end{aligned} \quad (11)$$

with the definitions $r \sin \theta e^{-\nu+\gamma} = e^\phi$, $e^{-\nu+\xi} = e^{\alpha-\beta}$ and the Lorentz factor $\Gamma \equiv (1 - U^2)^{-1/2}$. This differential equation needs to be solved numerically in combination with a 2-dimensional general relativistic stellar rotation code. The latter is used to determine the metric functions, frame dragging frequency, pressure and density gradients, and particle composition of a deformed neutron star as a function of its rotational frequency, $0 < \Omega \leq \Omega_K$. Depending on the cooling channels that are active at a given frequency, the numerical outcome of the rotation code serves as an input for the thermal evolution code, which is used to determine the luminosity, and thus the surface temperatures, of a deformed rotating neutron star. As mentioned in Sect. 3, because of stellar spin-down or spin-up, the density in the cores of rotating neutron stars may change dramatically so that new cooling channels open up (or close) with time. The changing cooling channels render the neutrino emissivities, heat capacities, and thermal conductivities rotation dependent, which alters the thermal response of the star. It is this response in the thermal behavior of rotating neutron stars that carries information about the properties of the matter in the dense baryonic stellar cores and possibly the deep crustal layers.

In passing we mention that the general relativistic equations of energy balance and thermal energy transport of non-rotating stars are given by

$$\frac{\partial(l e^{2\phi})}{\partial m} = -\frac{1}{\rho \sqrt{1 - 2m/r}} \left(\epsilon_\nu e^{2\phi} + c_\nu \frac{\partial(T e^\phi)}{\partial t} \right), \quad (12)$$

$$\frac{\partial(T e^\phi)}{\partial m} = -\frac{(l e^\phi)}{16\pi^2 r^4 \kappa \rho \sqrt{1 - 2m/r}}, \quad (13)$$

respectively [2]. Here, r is the distance from the center of the star, $m(r)$ is the mass, $\rho(r)$ is the energy density, $T(r, t)$ is the temperature, $l(r, t)$ is the luminosity, $\phi(r)$ is the gravitational potential, $\epsilon_\nu(r, T)$ is the neutrino emissivity, $c_\nu(r, T)$ is the specific heat, and $\kappa(r, T)$ is the thermal conductivity. The boundary conditions of Eqs. (12)

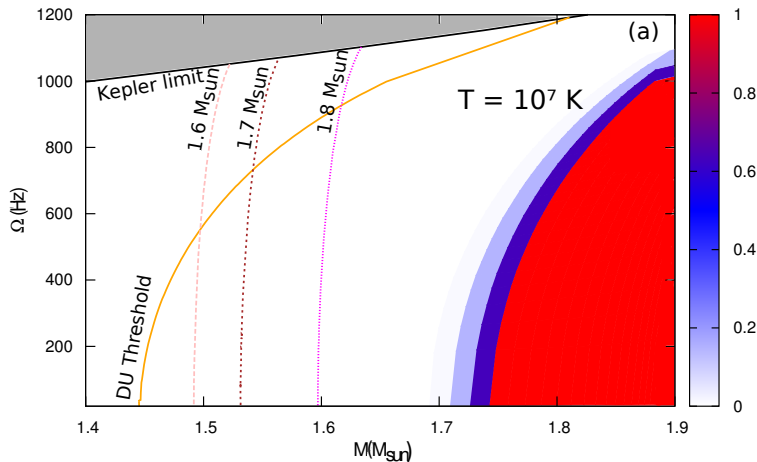


Figure 6: Direct Urca (DU) process in rotating neutron stars of gravitational mass M [36]. No stars are allowed above the curve labeled Kepler limit because of stellar mass shedding. The vertical curves show evolutionary tracks of isolated rotating neutron stars, whose baryon mass remain constant during spin-down. One sees that for several stars evolving along these tracks the DU process (see text) is not allowed at high rotation rates but becomes operative at lower rotation rates.

and (13) are determined by the luminosity at the stellar center and at the surface. The luminosity vanishes at the stellar center since there is no heat flux there. At the surface, the luminosity is defined by the relationship between the mantle temperature and the temperature outside of the star. Equations (12) and (13) have been solved numerically in [37] for hypothetical color-flavor-locked strange quark matter stars. It was found that such stars may undergo a significant reheating because of the magnetic recombination of rotational vortices, expelled from such stars during slow stellar spin-down.

The full 2-dimensional cooling equations of rotating neutron stars were solved recently in Ref. [38] for isolated rotating neutron stars. Driven by the loss of energy, such stars are gradually slowing down to lower frequencies, which increases the tremendous compression of the matter inside of them. This increase in compression changes both the global properties of rotating neutron stars as well as their hadronic core compositions. Both effects may register themselves observationally in the thermal evolution of such stars, as demonstrated in [36]. The rotation-driven particle process considered there was the direct Urca (DU) process $n \rightarrow p + e^- + \bar{\nu}_e$ which

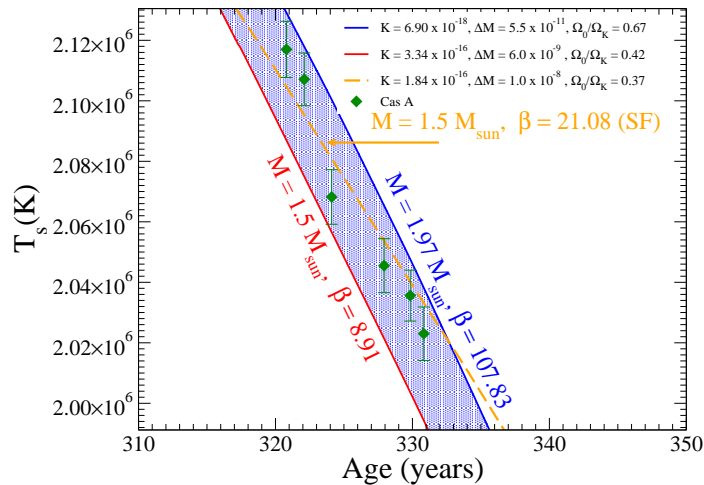


Figure 7: Cooling simulations reproducing the temperatures observed for the neutron star in Cas A over a ten-year period. ΔM denotes the mass of the accreted envelope, and Ω_0/Ω_K is the star's birth frequency relative to the Kepler frequency. Superfluidity and Pair-Breaking formation of nucleons is taken into account in the curve labeled SF.

becomes operative in neutron stars if the number of protons in the stellar core exceeds a critical limit of around 11% to 15% [39]. The neutrino luminosity associated with this reaction dominates over those of other neutrino emitting processes in the core [35, 39]. It was found that neutron stars spinning down from moderately high rotation rates of a few hundred Hertz may be creating just the right conditions where the DU process becomes operative (Fig. 6), leading to an observable effect (enhanced cooling) in the temperature evolution of such neutron stars. As it turned out (Fig. 7), the rotation-driven DU process could explain the unusual temperature evolution observed for the neutron star in Cas A, provided the mass of this neutron star lies in the range of 1.5 to 1.9 M_\odot and its rotational frequency at birth was between 40 (400 Hz) and 70% (800 Hz) of the Kepler (mass shedding) frequency, respectively [36].

Acknowledgment: This material is based upon work supported by the National Science Foundation under Grant No. 0854699. M. Orsaria thanks CONICET for financial support.

References

- [1] N. K. Glendenning, *Compact Stars, Nuclear Physics, Particle Physics, and General Relativity*, 2nd ed. (Springer-Verlag, New York, 2000).

- [2] F. Weber, *Pulsars as Astrophysical Laboratories for Nuclear and Particle Physics*, High Energy Physics, Cosmology and Gravitation Series (IOP Publishing, Bristol, Great Britain, 1999).
- [3] *Physics of Neutron Star Interiors*, ed. by D. Blaschke, N. K. Glendenning, and A. Sedrakian, Lecture Notes in Physics **578** (Spring-Verlag, Berlin, 2001).
- [4] J. M. Lattimer and M. Prakash, *Astrophys. J.* **550** (2001) 426.
- [5] F. Weber, *Prog. Part. Nucl. Phys.* **54** (2005) 193.
- [6] D. Page and S. Reddy, *Ann. Rev. Nucl. Part. Sci.* **56** (2006) 327.
- [7] T. Klähn *et al.*, *Phys. Rev. C* **74** (2006) 035802.
- [8] A. Sedrakian, *Prog. Part. Nucl. Phys.* **58** (2007) 168.
- [9] T. Klähn *et al.*, *Phys. Lett. B* **654** (2007) 170.
- [10] M. G. Alford, A. Schmitt, K. Rajagopal, and T. Schäfer, *Rev. Mod. Phys.* **80** (2008) 1455.
- [11] *Strongly Interacting Matter - The CBM Physics Book*, Lecture Notes in Physics **814**, 960 pages, (Springer, 2011).
- [12] NICA white paper, nica.jinr.ru/files/WhitePaper.pdf.
- [13] J. L. Friedman, J. R. Ipser, and L. Parker, *Astrophys. J.* **304** (1986) 115.
- [14] J. M. Lattimer, M. Prakash, D. Masak, and A. Yahil, *Astrophys. J.* **355** (1990) 241.
- [15] Y. Eriguchi, in: *Rotating objects and relativistic physics*, ed. by F. J. China and L. M. González-Romero (Springer-Verlag, Berlin, 1993).
- [16] M. Salgado, S. Bonazzola, E. Gourgoulhon, and P. Haensel, *Astron. & Astrophys.* **291** (1994) 155.
- [17] G. B. Cook, S. L. Shapiro, S. A. Teukolsky, *Astrophys. J.* **422** (1994) 227.
- [18] G. B. Cook, S. L. Shapiro, S. A. Teukolsky, *Astrophys. J.* **424** (1994) 823.
- [19] N. K. Glendenning and F. Weber, *Astrophys. J.* **400** (1992) 647.
- [20] N. K. Glendenning, *Phys. Rev. D* **46** (1992) 4161.
- [21] J. W. T. Hessels, S. M. Ransom, I. H. Stairs, P. C. C. Freire, V. M. Kaspi, and F. Camilo, *Science* **311** (2006) 1901.

- [22] D. C. Backer, S. R. Kulkarni, C. Heiles, M. M. Davis, and W. M. Goss, *Nature* **300** (1982) 615.
- [23] A. S. Fruchter, D. R. Stinebring, and J. H. Taylor, *Nature* **334** (1988) 237.
- [24] N. K. Glendenning, S. Pei, and F. Weber, *Phys. Rev. Lett.* **79** (1997) 1603.
- [25] F. Weber and P. Rosenfield, *Rotating neutron stars*, Proceedings of HYP 2006, ed. by J. Pochodzalla and Th. Walcher (Springer, Berlin, 2007) p. 381.
- [26] F. Weber, R. Negreiros, P. Rosenfield, and M. Stejner, *Prog. Part. Nucl. Phys.* **59** (2007) 94.
- [27] M. Alford, D. Blaschke, A. Drago, T. Klähn, G. Pagliara, J. Schaffner-Bielich, *Quark matter and the masses and radii of compact stars*, (astro-ph/0606524).
- [28] M. Orsaria, H. Rodrigues, F. Weber, and G. A. Contrera, *Phys. Rev. D* **87** (2013) 023001.
- [29] N. K. Glendenning, *Phys. Rev. D* **46** (1992) 1274.
- [30] N. K. Glendenning, *Phys. Rep.* **342** (2001) 393.
- [31] K. Masuda, T. Hatsuda and T. Takatsuka, [arXiv:1205.3621](https://arxiv.org/abs/1205.3621) [nucl-th].
- [32] C. H. Lenzi and G. Lugones, *Astrophys. J.* **759** (2012) 57.
- [33] D. B. Blaschke, D. Gomez Dumm, A. G. Grunfeld, T. Klähn, and N. N. Scoccola, *Phys. Rev. C* **75** (2007) 065804.
- [34] Z. Zhang and T. Kunihiro, *Phys. Rev. D* **80** (2009) 014015.
- [35] D. Page, U. Geppert, and F. Weber, *Nucl. Phys. A* **777** (2006) 492.
- [36] R. Negreiros, S. Schramm, and F. Weber, *Phys. Lett. B* **718** (2013) 1176.
- [37] B. Niebergal, R. Ouyed, R. Negreiros, and F. Weber, *Phys. Rev. D* **81** (2010) 043005.
- [38] R. Negreiros, S. Schramm, and F. Weber, *Phys. Rev. D* **85** (2012) 104019.
- [39] J. M. Lattimer, C. J. Pethick, M. Prakash, and P. Haensel, *Phys. Rev. Lett.* **66** (1991) 2701.